

1 **Title.** A computational model for learning from repeated trauma

2 **Authors.** Alfred P. Kaye^{1,2}, Alex C. Kwan^{1,3}, Kerry J. Ressler^{4,5}, John H. Krystal^{1,2}

3 1. Yale University Department of Psychiatry, New Haven, CT

4 2. VA National Center for PTSD Clinical Neuroscience Division, West Haven, CT

5 3. Yale University Department of Neuroscience, New Haven, CT

6 4. McLean Hospital, Division of Depression and Anxiety Disorder, Belmont, MA

7 5. Harvard Medical School, Department of Psychiatry, Boston, MA

8

9 **Abstract.** Traumatic events can lead to lifelong inflexible adaptations in threat
10 perception and behavior which characterize posttraumatic stress disorder (PTSD). This
11 process involves associations between sensory cues and internal states of threat and
12 then generalization of the threat responses to previously neutral cues. However, most
13 formulations neglect adaptations to threat that are not specific to those associations. In
14 order to incorporate non-associative responses to threat, we propose a computational
15 theory of PTSD based on adaptation to the frequency of traumatic events using a
16 reinforcement learning momentum model. Recent threat prediction errors generate
17 momentum that influences subsequent threat perception in novel contexts. This model
18 fits data acquired from a mouse model of PTSD, in which unpredictable footshocks in
19 one context accelerate threat learning in a novel context. The theory is also consistent
20 with epidemiological data showing that PTSD incidence increases with the number of
21 traumatic events, as well as the disproportionate impact of early life trauma. Since the
22 theory proposes that PTSD relates to the average of recent threat prediction errors

23 rather than the strength of a specific association, it makes novel predictions for the
24 treatment of PTSD.

25

26 **Introduction**

27 Computational psychiatry seeks to define psychiatric disorders in terms of
28 fundamental algorithms for survival rather than only as pathological states (1-3).
29 Quantitative models may allow personalization of mental health care, insight into the
30 nature of the disorder, inform neurobiological investigations into psychiatric disorders, or
31 predict the trajectory of symptoms (4-6). For example, depression has been conceived
32 as an adaptation to periods of low reward availability (7). Similarly, hallucinations have
33 been conceptualized as resulting from excessive weighting of prior expectations for
34 auditory stimuli in a Bayesian model (8-9). One approach to describing a computational
35 function of a neural system is using David Marr's three levels of analysis (10) (Figure
36 1A), which seeks to map connections between computational goals, algorithmic
37 procedures to achieve them, and the neurobiological substrate underlying these
38 processes.

39 Posttraumatic stress disorder has a computational description that organizes
40 theory and neurobiological data across Marr's three levels - associative fear learning
41 (Figure 1B, refs. 11-15). Learning models have been successfully applied to PTSD and
42 underlie current conceptualizations of the disorder and treatment options (16-17). PTSD
43 is seen as an extreme outcome of associative fear learning, which in turn is a
44 fundamental mechanism for predicting threats based on previous experience (18). In
45 this model, PTSD occurs when life-threatening situations create potent associations

46 between sensory reminders of the traumatic event and the emotional experience of fear
47 (17). The intensity of this association then motivates a person to avoid (19) future
48 trauma cues, limits extinction of the fear memory (20), and supports the subsequent
49 formation of new fear memories via generalization and second-order conditioning (21).
50 This process can be described mathematically, enabling learning parameters to be
51 precisely measured during new associative learning in a laboratory setting (18). The
52 precision with which associative learning can be controlled has enabled neurobiological
53 studies into circuit mechanisms in both humans and animals (22).

54 In contrast, non-associative learning – increases (sensitization) or decreases
55 (habituation) in response to a repeated stimulus (23) – is a prominent component of
56 PTSD that lacks a formal algorithmic description (Figure 1B). In humans, repeated
57 traumatic events increase the probability of developing PTSD and may change the
58 nature of the disorder (24-25). Core PTSD symptoms, such as hyperarousal, inherently
59 involve an exaggerated response to sensory cues – importantly, these cues need not be
60 associated with the traumatic event to trigger the response (26) but may instead result
61 from sensitization of neuromodulatory systems (27-28). Neurobiological studies in
62 animals have shown that stress enhances both innate defensive behaviors (29) and
63 learning about unrelated fear cues (30). There are conceptual models of how
64 habituation and sensitization occur (Dual Process Theory, ref. 31; Wagner-Koniorsky
65 Theory, ref. 32), which center the role of arousal in changing the response to a stimulus
66 with repetition. However, these models lack the algorithmic detail and clear relation to
67 survival value of Rescorla-Wagner and related reinforcement learning (RL) models (33).

68 This has limited the ability to parametrically manipulate and therefore understand non-
69 associative learning in PTSD patients and animal models.

70 Here, we posit an ecological role for non-associative learning in estimating the
71 frequency of predator attacks (or other violence). We then apply a Bayesian approach
72 to understand how well an ideal agent could estimate predation risk from its own life
73 history. We show that a natural consequence of this approach is that early life trauma
74 has disproportionate impact on estimated risk even when controlling for the number of
75 traumatic events. After describing the behavior of such an ideal Bayesian agent, we turn
76 to a recently developed RL model (7, 34-36) in order to integrate associative and non-
77 associative learning. Non-associative learning becomes more important as traumas
78 occur in more different contexts and less distant times. The RL model points towards
79 novel interventions and future neurobiological approaches to improve PTSD symptoms.

80

81 **Methods**

82 **Models of threat estimation.** Two models of threat estimation are identified and
83 compared: (1) a Bayesian model, in which an agent experiences events (attacks) and
84 attempts to estimate the frequency of those attacks and (2) a reinforcement learning
85 agent, which experiences events (attacks) in contexts (all attacks occur in different
86 contexts) over time and must estimate the threat in each environment. The
87 reinforcement learning model is then compared with behavioral data for a mouse
88 undergoing a stress procedure.

89 **Bayesian attack model.** At each time step, events (attacks) are binomially
90 distributed with probability of attack p_a for 700 time steps (Figure 2a). Deaths occur with

91 probability p_d contingent on an attack occurring. The agent's estimate of p_a and p_d is
92 derived from the sequence of attack observations ($x_t = 0,0,1 \dots 0$) according to Bayes'
93 rule

$$94 \quad p(p_a, p_d | \mathbf{x}_t) = \frac{p(\mathbf{x}_t | p_a, p_d) p(p_a, p_d)}{\int p(\mathbf{x}_t | p_a, p_d) dx_t} \quad (1)$$

95 using a Markov Chain Monte Carlo sampler with a flat prior at time $t=0$. Specifically, an
96 affine invariant ensemble MCMC sampler (MCMC Hammer, ref. 37) toolbox for Matlab
97 with 31 walkers was used to estimate the posterior. For subsequent timepoints,
98 Bayesian estimation is performed with the prior distribution as the posterior of the
99 previous time step.

100 Autocorrelated attack rate time series were generated for an AR(1)
101 autoregressive process

$$102 \quad p_{a,t} = cp_{a,t-1} + \mathcal{N}(0,0.1), \quad (2)$$

103 where $p_{a,t}$ is the attack rate at time t , c is a constant equal to the correlation of
104 successive time steps, and $\mathcal{N}(\mu, \sigma)$ is normally distributed noise with mean μ and
105 standard deviation σ . Simulations used the arima function in Matlab. $N=10,000$
106 simulated lifetime attack rate time series were generated, then for each an agent's
107 experienced attack time series was generated and the MCMC Hammer estimator was
108 then used to progressively estimate attack rates as above.

109 **Reinforcement learning models.** In temporal difference learning, threat at time t in
110 context c ($T_{c,t}$) is learned from a sequence of unconditioned stimuli (u_t) which produce
111 prediction errors according to

$$112 \quad T_{c,t} = T_{c,t-1} + \alpha(u_t - \gamma_1 T_{c,t-1}), \quad (3)$$

113 where α is a learning rate and γ_1 is a decay rate constant. Equation 3 is referred to as
114 RL model in the Results section, and describes the formation of associative threat
115 learning. The addition of a momentum term (7) allows prediction errors from different
116 states to influence one another according to an RL momentum model

$$117 \quad T_{c,t} = T_{c,t-1} + \alpha(u_t - c_1 T_{c,t-1}) + f m_t, \quad (3)$$

118 where f is a scaling constant and m_t is the momentum at time t . This momentum term is
119 defined by

$$120 \quad m_t = m_{t-1} + \gamma_2 \sum_{c=\{A,B,\dots\}} \alpha(u_t - T_{c,t-1}) \quad (4)$$

121 in which the sum of decayed prediction errors across all contexts $c = \{A, B, \dots\}$ with
122 momentum decay constant γ_2 . This can lead to either oscillatory behavior or slow
123 summation of prediction errors across states depending on γ_2 . Reinforcement learning
124 models (RL – equation 3, RL with momentum – equation 4) were fit to smoothed
125 freezing (sliding window, 15s) on days 1, 6, and 7. Inputs to the model were shock times
126 and threat was fit for both Context A and Context B. Parameters for each model were fit
127 using maximum likelihood estimation in Matlab. Maximum likelihood fit was compared
128 by calculating the Bayes Information Criterion (BIC) for RL and RL with momentum
129 models at the single animal level for both stressed and unstressed mice.

130 **Stress enhanced fear learning.** All procedures were carried out in accordance with the
131 ethical guidelines of the National Institutes of Health and were approved by the
132 Institutional Animal Care & Use Committee of Yale University. 8-12 week old C57Bl/6
133 male mice were stressed using using the Stress-Enhanced Fear Learning model (30),
134 which has been shown to lead to long-lasting enhancement of fear and anxiety
135 behaviors in both mice (30) and rats (38). This model consists of 15 unpredictable

136 footshocks (1mA, 1s) with random intershock intervals between 4 and 8 minutes. For
137 contextual fear experiments, a second context (Context B) was used on day 6, in a
138 separate room with different ambient auditory, visual, tactile, and olfactory
139 characteristics. On Day 6, a single 1mA 1s shock was administered after 5 minutes, and
140 then freezing was assessed for 5 more minutes. On day 7, mice were returned to
141 Context B for 10 minutes. MedAssociates boxes were used for all footshock
142 experiments, and freezing was assessed as complete cessation of movement other
143 than breathing (motion <18 a.u.) with automated VideoFreeze software.

144

145 **Results**

146 Previous approaches to computational modeling of PTSD have focused on
147 defining changes in associative learning after traumatic experience (11-15). PTSD is
148 thus framed as a consequence of underlying mechanisms for predicting threat based on
149 previous *associations*. In contrast, we were interested in whether PTSD might arise
150 from an agent estimating the *frequency* of threat exposure. In order to determine how
151 an ideal observer would estimate the frequency of threat exposure, we first posit a
152 simplified model of exposure to repeated traumatic events. By constructing an ideal
153 Bayesian observer of these traumatic events, we establish a baseline for what can be
154 inferred from repeated events without association. We then turn to a recently developed
155 reinforcement learning model (7, 34-36) to integrate non-associative learning (about the
156 frequency of threat) with associative learning (about the associations of threat). Finally,
157 we fit the reinforcement learning model to data derived from mice undergoing Stress-
158 enhanced Fear Learning (SEFL), a rodent model of PTSD (30). We then consider the

159 implications of our findings for treatment and future research into the neurobiology of
160 PTSD.

161 **Model 1 – PTSD as trauma rate estimation**

162 An organism must estimate the threat of violence to adapt to it. This process of
163 estimation must necessarily involve information gathered across timescales, since
164 threat may increase suddenly or may increase over long periods (39). Longer timescale
165 estimation of threat involves integrating experience in disparate environments.

166 To consider a concrete example: predator attacks are events which carry a
167 significant probability of death (20% for mice exposed to an owl, ref. 40). If the
168 probability of death is high, then the animal will experience few attacks before dying
169 (Figure 2B). In this information-poor environment, the animal must maximize the
170 available information in estimating the rate of such attacks. In order to determine how
171 well an ideal observer could do under such conditions, we constructed a simple
172 probabilistic model with a fixed probability of attacks p_a and probability of dying per
173 attack p_d at each time point (Figure 2A). Using a Markov Chain Monte Carlo sampler,
174 we were able to estimate the posterior distribution of p_a (Figure 2C), which makes it
175 possible to identify the estimate available to a Bayesian observer. As expected,
176 variance in p_a decreases progressively over the lifetime of the agent as more samples
177 become available (Figure 2D).

178 The disproportionate impact of early life stress (ELS) on adult behavior (39) is
179 explained by the Bayesian trauma rate model. Childhood traumatic experiences have a
180 strong impact on adult brain structure and function (41). Life History Theory explains
181 this by positing that stressful experiences in childhood provide information about

182 organismal strategies that will be adaptive in the adult environment (42). We evaluated
183 the Bayesian trauma rate estimator in two scenarios with the same total number of
184 traumatic events, one in which traumas occur early in life (ELS) and one in which they
185 are spread across the lifespan (Figure 3A). Variance in \hat{p}_a decreases with time in both
186 models, as traumatic events reduce uncertainty in the true rate of violence (Figure 3B).
187 However, over the course of the lifespan the ELS model shows a higher estimated rate
188 of violence (\hat{p}_a). Thus, the increased response to ELS does not require specialized
189 critical period mechanisms, but instead arises naturally in a normative estimator of
190 violence rate.

191 **Model 2 – PTSD as threat momentum**

192 Normative Bayesian models can explain the performance of an ideal behavior,
193 but are difficult to implement in biological systems due to the computational difficulty in
194 integrating probability distributions to find the posterior (43). It can therefore be useful to
195 define more biologically plausible models which can then be compared to the
196 performance of the ideal Bayesian observer (37). Reinforcement learning (RL) is a
197 flexible class of models that can be used to learn in real time from experience. Unlike
198 Bayesian models, RL involves updating stored values of stimuli or actions based on set
199 learning rules. Parameters of RL models can then be fit to empirical behavioral data of
200 animals or human subjects, to derive differences in parameters between groups. RL
201 models can also be used to explain learning processes, or to identify neural processes
202 that map onto learning processes.

203 In this section, we propose that a recently proposed RL momentum model (7, 34-
204 36) can explain features of PTSD not explained by classical associative learning

205 models. Traumatic events may come in clusters, so learning from trauma involves
206 combining information from distinct experiences that occur close in time. The
207 momentum model as applied to neuropsychiatric disorders suggests that a common
208 tendency, or mood, may underlie motivated behaviors over a period of time. For intuition
209 into the reason why traumatic events occur together, consider an agent subject to
210 predation risk. Empirical measurements of predator-prey interactions confirm the
211 existence of large fluctuations in predator number (39), which are also predicted by
212 mathematical models of predator-prey interactions such as the Lotka-Volterra
213 equations. In order to adapt to time-varying predator rates, an organism must be
214 capable of tracking the rate of attacks it experiences.

215 Classical RL models, such as temporal difference learning (Figure 4A), enable an
216 organism to associate threatening experiences with the context in which they are
217 experienced. However, threats in one context do not influence threats in another (Figure
218 4A). In contrast, in the RL-momentum model, traumatic events occurring close in time
219 but in unrelated environments contribute to a slowly varying momentum term (Figure
220 4B), which can be thought of as a pervasive mood biasing subsequent experience.
221 Momentum carries information about recent threats, allowing the agent to correctly
222 assess risk in a changing environment. The ideal length of time for momentum to persist
223 depends on how long threats persist (Figure 4C). When attacks are uncorrelated in
224 time, there is no advantage to momentum and the optimal momentum learning rate
225 (highest correlation to the underlying threat rate) is zero, reducing the RL momentum
226 model to a classical RL model. When attacks are correlated (Figure 4C, light blue), a
227 substantial improvement in threat estimation can be obtained by including the

228 momentum parameter. The long-time scale of optimal threat adaptation offers a
229 potential explanation for the persistence of PTSD symptoms. If threat momentum, rather
230 than the specific association with the initial traumatic event, were the source of PTSD
231 symptoms, then this would have substantial implications for the understanding of PTSD.

232 To test this idea, we induced stress in a mouse model of PTSD (Stress-
233 Enhanced Fear Learning; SEFL) and compared the performance of temporal difference
234 learning (RL model) and a momentum model (RL momentum model) in explaining
235 defensive behavior (Figure 5). In this model, mice receive unpredictable footshocks in
236 one context (Context A) and then show sensitized threat responses to a single
237 footshock in another context (Context B) later (Figure 5A, top). The RL momentum
238 model fits the observed freezing behavior (Figure 5A, bottom) well, showing a
239 disproportionate freezing response to the single footshock in a novel context. This
240 sensitized freezing behavior can be explained by the momentum term in the model,
241 which links the threat prediction errors produced across contexts.

242 We compared Maximum Likelihood fits between the RL and RL momentum
243 models (n=18 unstressed, n=17 stressed mice), using the Bayes Information Criteria
244 (BIC; Figure 5B). When the momentum learning parameter (ν) is zero, the two models
245 are equivalent, but the the RL momentum model has a greater number of parameters (4
246 for RL momentum, 2 for RL model). Since the BIC penalizes the number of parameters,
247 this produces model fits where the RL model is preferred (for unstressed mice, RL
248 model was preferred in 17/18 animals). For stressed mice, however, the BIC strongly
249 favored fits from the RL momentum model (14/17 animals). The RL momentum model

250 predicts greater freezing in a novel context in stressed animals than the RL model,
251 which accounts for the improved predictions over the RL model.

252 The RL-momentum model of PTSD presents an additional learning mechanism
253 by which PTSD symptoms may be ameliorated. In the classical RL model of PTSD,
254 extinction learning (Figure 6A) works to reduce PTSD by generating small prediction
255 errors when the agent is re-exposed to the traumatic context. This approach underlies
256 evidence-based psychological therapies for PTSD, such as prolonged exposure and
257 cognitive reprocessing therapy. The RL momentum model retains extinction of learned
258 associations, but the threat prediction errors generated by extinction also generate
259 negative momentum that reduces responses to novel threats (Figure 6B). This model
260 also offers a novel perspective on treatment failure of exposure therapy in PTSD.

261 Current learning-based accounts of this phenomenon posit that individuals may
262 experience extinction renewal or extinction resistance, in which either extinction fails to
263 occur or in which the extinction memory may be specific to the context in which it was
264 generated (e.g., the therapy session). In contrast, the RL momentum proffers a simple
265 explanation – unrelated mild stressors generate threat momentum, which increases
266 threat associated with the original traumatic context (Figure 6C). Similarly, an
267 implication of this model is that exposure to novel threats independent of the traumatic
268 context could reduce threat momentum. For example, an agent encountering an intense
269 innate threat (e.g., standing on the side of a high cliff) without injury might experience a
270 strong negative prediction error which would reduce threat momentum for the same
271 reason as exposure to a cue associated to a traumatic event.

272 **Discussion**

273 We formulated PTSD as a learning process directed at estimating the rate of
274 trauma rather than the specific associations with the trauma. The Bayesian formulation
275 of this problem treated the agent experiencing trauma as an ideal observer. We found
276 that the rate of traumatic events could be estimated well by this agent. Early life trauma
277 had disproportionate impact in this model even without specialized mechanisms for
278 amplifying early life experience. We applied the reinforcement learning momentum
279 model to PTSD, and found that RL-momentum performs well when violence is clustered
280 in time. The slower the change in trauma rate, the more momentum contributes to
281 optimal learning from traumatic stress. This model also offers a novel conceptualization
282 of extinction learning, and suggests that exposure to unassociated strong threats could
283 affect threat momentum. Understanding the impact of innate danger on threat
284 momentum requires further modeling and empirical investigation, since exposure to
285 innate threat could lead to either positive or negative changes in threat momentum.

286 Previous formal approaches to learning in PTSD have focused primarily on
287 associative mechanisms. However, experimental observations of sensitization to new
288 threats by previous stress are often used to model PTSD (26,29-30). We show that
289 stress sensitization of threat, a model of PTSD, is well fit by the RL-momentum model.
290 However, our ability to precisely fit the parameters of the RL-momentum model is
291 limited by the binary nature of the stress in this dataset. Full validation and parameter-
292 fitting for the RL-momentum model will require more precise manipulations of the
293 sequence of threat prediction errors over time.

294 A further limitation of this study is that we did not consider parameter regimes
295 that may give rise to habituation (decrease in response to repeated stimuli). Both

296 sensitization and habituation can occur in the RL-momentum model, depending on
297 chosen parameters (7). In PTSD, habituation has recently been suggested as an
298 outcome of repeated trauma (44), and may relate to the numbing symptoms in PTSD.
299 Habituation and sensitization have been thought of as separate processes which
300 competitively modulate responses to repeated stimuli (45). PTSD involves both
301 excessive (hyperarousal) and decreased (numbing) emotional reactions occur after
302 traumatic stress (45-47). A more complete model of the impact of a sequence of threat
303 prediction errors on subsequent emotional responses may explain this apparent
304 contradiction.

305 Future progress in understanding the role of non-associative learning in PTSD
306 may depend on measuring the neural substrate of threat momentum (or estimated
307 attack rate in the Bayesian model). Applying David Marr's three levels of analysis to
308 non-associative learning from threat (Figure 1), we have defined the computational
309 problem ("predicting future threats based on a sequence of attacks") that must be
310 solved. We have compared two algorithms for accomplishing this goal: Bayesian MCMC
311 sampling and RL momentum. We find the RL momentum model offers a formal
312 mathematical approach at the implementation level which explains clinical features of
313 PTSD and behavior in a mouse model of PTSD. However, the implementation level of
314 the RL momentum has not been identified.

315 Identifying PTSD with threat momentum may facilitate future neurobiological and
316 translational studies of PTSD. Extensive work has shown that patients with PTSD have
317 different learning rate parameters during fear and extinction learning (11-15) than
318 controls in the formation of associations. This study extends these findings by offering a

319 model of how the sequence of threat prediction errors may generate other associative
320 learning alterations in PTSD. The neurobiological correlates of threat momentum would
321 be slowly varying summing functions of previous threat prediction errors which sensitize
322 defensive behaviors, such as neuromodulatory systems (29) or molecular switches
323 leading to persistent neural changes (48). Future extensions of this approach may link
324 effects of arousal on learning rates (rather than overall threat) to averaged recent threat
325 prediction errors, similar to Pearce-Hall learning (49). Thus, the present study may
326 facilitate future work linking non-associative and associative mechanisms in PTSD.
327 Such links are evident in behavioral and epidemiological data and have plausible
328 biological mechanisms, but have previously lacked a computational model to facilitate
329 the design of future experiments.

330

331 References

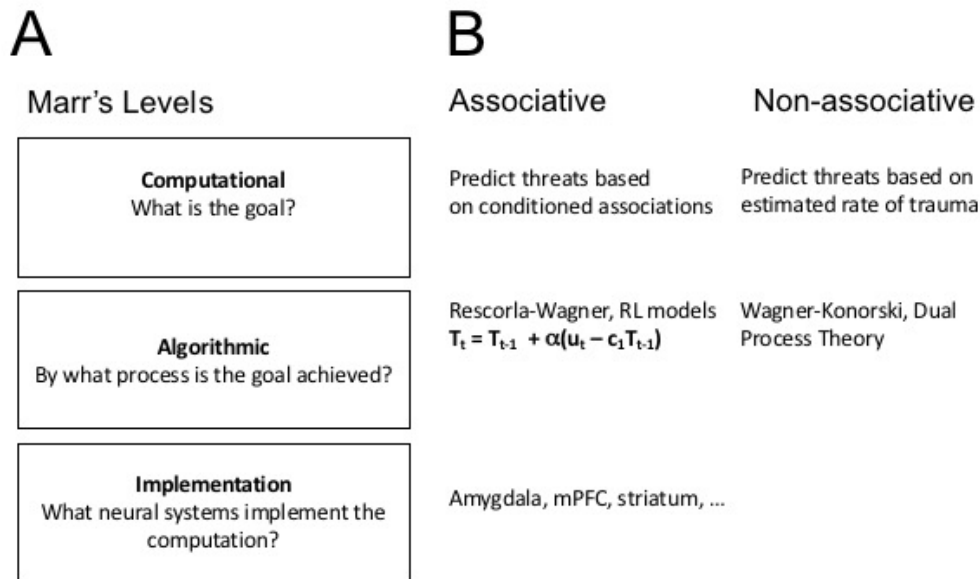
332

- 333 1. Montague, P.R., Dolan, R.J., Friston, K.J., and Dayan, P. (2012). Computational
334 psychiatry. *Trends in Cognitive Sciences* 16, 72–80.
- 335 2. Wang, X.-J., and Krystal, J.H. (2014). Computational Psychiatry. *Neuron* 84, 638–
336 654.
- 337 3. Bach, D.R., and Dayan, P. (2017). Algorithms for survival: a comparative perspective
338 on emotions. *Nature Reviews Neuroscience* 18, 311–319.
- 339 4. Galatzer-Levy, I.R., Karstoft, K.-I., Statnikov, A., and Shalev, A.Y. (2014).
340 Quantitative forecasting of PTSD from early trauma responses: a Machine Learning
341 application. *J Psychiatr Res* 59, 68–76.
- 342 5. Galatzer-Levy, I.R., Ma, S., Statnikov, A., Yehuda, R., and Shalev, A.Y. (2017).
343 Utilization of machine learning for prediction of post-traumatic stress: a re-examination
344 of cortisol in the prediction and pathways to non-remitting PTSD. *Transl Psychiatry* 7,
345 e1070.
- 346 6. Saxe, G.N., Ma, S., Ren, J., and Aliferis, C. (2017). Machine learning methods to
347 predict child posttraumatic stress: a proof of concept study. *BMC Psychiatry* 17, 223.
- 348 7. Eldar, E., Rutledge, R.B., Dolan, R.J., and Niv, Y. (2016). Mood as Representation of
349 Momentum. *Trends in Cognitive Sciences* 20, 15–24.
- 350 8. Fletcher, P.C., and Frith, C.D. (2009). Perceiving is believing: a Bayesian approach to
351 explaining the positive symptoms of schizophrenia. *Nature Reviews Neuroscience* 10,
352 48–58.
- 353 9. Powers, A.R., Mathys, C., and Corlett, P.R. (2017). Pavlovian conditioning–induced
354 hallucinations result from overweighting of perceptual priors. *Science* 357, 596–600.
- 355 10. Marr, D. (2010). *Vision: A Computational Investigation Into the Human*
356 *Representation and Processing of Visual Information* (MIT Press).
- 357 11. Jovanovic, T., Kazama, A., Bachevalier, J., and Davis, M. (2012). Impaired safety
358 signal learning may be a biomarker of PTSD. *Neuropharmacology* 62, 695–704.
- 359 12. Yehuda, R., Keefe, R.S.E., Harvey, P.D., Levengood, R.A., Gerber, D.K., Geni, J.,
360 and Siever, L.J. (1995). Learning and memory in combat veterans with posttraumatic
361 stress disorder. *The American Journal of Psychiatry* 152, 137–139.
- 362 13. Homan, P., Levy, I., Feltham, E., Gordon, C., Hu, J., Li, J., Pietrzak, R.H.,
363 Southwick, S., Krystal, J.H., Harpaz-Rotem, I., et al. (2019). Neural computations of
364 threat in the aftermath of combat trauma. *Nature Neuroscience* 22, 470.
- 365 14. Brown, V.M., Zhu, L., Wang, J.M., Frueh, B.C., King-Casas, B., and Chiu, P.H.
366 Associability-modulated loss learning is increased in posttraumatic stress disorder. *eLife*
367 7.
- 368 15. Ross, M.C., Lenow, J.K., Kilts, C.D., and Cisler, J.M. (2018). Altered neural
369 encoding of prediction errors in assault-related posttraumatic stress disorder. *J*
370 *Psychiatr Res* 103, 83–90.
- 371 16. Foa, E.B. (2011). Prolonged exposure therapy: Past, present, and future.
372 *Depression and Anxiety* 28, 1043–1047.
- 373 17. Jaycox, L.H., Foa, E.B., and Morral, A.R. (1998). Influence of emotional
374 engagement and habituation on exposure therapy for PTSD. *Journal of Consulting and*
375 *Clinical Psychology* 66, 185–192.

- 376 18. Rescorla, R.A., & Wagner, A.R. (1972). A theory of Pavlovian conditioning: variations
377 in the effectiveness of reinforcement and non reinforcement. In AH. Black & W.F.
378 Prokasy (eds.), *Classical conditioning II: current research and theory* (pp. 64-99) New
379 York: Appleton-Century-Crofts.
- 380 19. Asmundson, G.J.G., Stapleton, J.A., and Taylor, S. (2004). Are avoidance and
381 numbing distinct PTSD symptom clusters? *Journal of Traumatic Stress* 17, 467–475.
- 382 20. Izquierdo, A., Wellman, C.L., and Holmes, A. (2006). Brief Uncontrollable Stress
383 Causes Dendritic Retraction in Infralimbic Cortex and Resistance to Fear Extinction in
384 Mice. *J. Neurosci.* 26, 5733–5738.
- 385 21. Beck, J.G., and Sloan, D.M. (2012). *The Oxford Handbook of Traumatic Stress*
386 *Disorders* (Oxford University Press, USA).
- 387 22. Maddox, S.A., Hartmann, J., Ross, R.A., and Ressler, K.J. (2019). Deconstructing
388 the Gestalt: Mechanisms of Fear, Threat, and Trauma Memory Encoding. *Neuron* 102,
389 60–74.
- 390 23. Thompson, R.F., and Spencer, W.A. (1966). Habituation: A model phenomenon for
391 the study of neuronal substrates of behavior. *Psychological Review* 73, 16–43.
- 392 24. Khoury, L., Tang, Y.L., Bradley, B., Cubells, J.F., and Ressler, K.J. (2010).
393 Substance use, childhood traumatic experience, and Posttraumatic Stress Disorder in
394 an urban civilian population. *Depression and Anxiety* 27, 1077–1086.
- 395 25. Almli, L.M., Mercer, K.B., Kerley, K., Feng, H., Bradley, B., Conneely, K.N., and
396 Ressler, K.J. (2013). ADCYAP1R1 genotype associates with post-traumatic stress
397 symptoms in highly traumatized African-American females. *American Journal of Medical*
398 *Genetics Part B: Neuropsychiatric Genetics* 162, 262–272.
- 399 26. Morgan, C.A., Grillon, C., Southwick, S.M., Davis, M., and Charney, D.S. (1995).
400 Fear-potentiated startle in posttraumatic stress disorder. *Biological Psychiatry* 38, 378–
401 385.
- 402 27. Pietrzak, R.H., Gallezot, J.-D., Ding, Y.-S., Henry, S., Potenza, M.N., Southwick,
403 S.M., Krystal, J.H., Carson, R.E., and Neumeister, A. (2013). Association of
404 Posttraumatic Stress Disorder With Reduced In Vivo Norepinephrine Transporter
405 Availability in the Locus Coeruleus. *JAMA Psychiatry* 70, 1199–1205.
- 406 28. Kelmendi, B., and Southwick, S.M. (2018). Locus Coeruleus Hyperactivity in
407 Posttraumatic Stress Disorder: Answers and Questions. *Biological Psychiatry* 83, 197–
408 199.
- 409 29. Li, L., Feng, X., Zhou, Z., Zhang, H., Shi, Q., Lei, Z., Shen, P., Yang, Q., Zhao, B.,
410 Chen, S., et al. (2018). Stress Accelerates Defensive Responses to Looming in Mice
411 and Involves a Locus Coeruleus-Superior Colliculus Projection. *Current Biology* 28,
412 859–871.e5.
- 413 30. Rau, V., DeCola, J.P., and Fanselow, M.S. (2005). Stress-induced enhancement of
414 fear learning: An animal model of posttraumatic stress disorder. *Neuroscience &*
415 *Biobehavioral Reviews* 29, 1207–1223.
- 416 31. Groves, P.M., and Thompson, R.F. (1970). Habituation: A dual-process theory.
417 *Psychological Review* 77, 419–450.
- 418 32. Wagner A.R. (1979). Habituation and memory. In: Dickinson A, Boakes RA,
419 editors. *Mechanisms of learning and motivation: A memorial volume for Jerry*
420 *Konorski*. Lawrence Earlbaum Assoc.; Hillsdale, NJ. pp. 53–82.

- 421 33. Sutton, R.S., and Barto, A.G. (2018). Reinforcement Learning: An Introduction (MIT
422 Press).
- 423 34. Rutledge, R.B., Skandali, N., Dayan, P., and Dolan, R.J. (2014). A computational
424 and neural model of momentary subjective well-being. *Proc Natl Acad Sci U S A* 111,
425 12252–12257.
- 426 35. Eldar, E., and Niv, Y. (2015). Interaction between emotional state and learning
427 underlies mood instability. *Nat Commun* 6, 6149.
- 428 36. Trapp, S., O’Doherty, J.P., and Schwabe, L. (2018). Stressful Events as Teaching
429 Signals for the Brain. *Trends Cogn. Sci. (Regul. Ed.)* 22, 475–478.
- 430 37. Akeret, J., Seehars, S., Amara, A., Refregier, A., and Csillaghy, A. (2013).
431 CosmoHammer: Cosmological parameter estimation with the MCMC Hammer.
432 *Astronomy and Computing* 2, 27–39.
- 433 38. Sillivan, S.E., Joseph, N.F., Jamieson, S., King, M.L., Chévere-Torres, I., Fuentes,
434 I., Shumyatsky, G.P., Brantley, A.F., Rumbaugh, G., and Miller, C.A. (2017).
435 Susceptibility and Resilience to Posttraumatic Stress Disorder-like Behaviors in Inbred
436 Mice. *Biol. Psychiatry* 82, 924–933.
- 437 39. Pavlůvčík, P., Poprach, K., Machar, I., Losík, J., Gouveia, A., and Tkadlec, E.
438 (2015). Barn Owl Productivity Response to Variability of Vole Populations. *PLoS One*
439 10.
- 440 40. Ilany, A., and Eilam, D. (2008). Wait before running for your life: defensive tactics of
441 spiny mice (*Acomys cahirinus*) in evading barn owl (*Tyto alba*) attack. *Behav Ecol*
442 *Sociobiol* 62, 923–933.
- 443 41. Callaghan, B.L., and Tottenham, N. (2016). The Stress Acceleration Hypothesis:
444 effects of early-life adversity on emotion circuits and behavior. *Current Opinion in*
445 *Behavioral Sciences* 7, 76–81.
- 446 42. Frankenhuys, W.E., and de Weerth, C. (2013). Does Early-Life Exposure to Stress
447 Shape or Impair Cognition? *Curr Dir Psychol Sci* 22, 407–412.
- 448 43. Pouget, A., Beck, J.M., Ma, W.J., and Latham, P.E. (2013). Probabilistic brains:
449 knowns and unknowns. *Nature Neuroscience* 16, 1170–1178.
- 450 44. Stevens, J., Ressler, K., and Jovanovic, T. (2018). T22. PTSD Symptom Profiles
451 and Amygdala Function Vary as a Function of Repeated Trauma Exposure: Numbing as
452 a Specific Neurobiological Phenotype. *Biological Psychiatry* 83, S137.
- 453 45. Hopper, J.W., Frewen, P.A., Kolk, B.A. van der, and Lanius, R.A. (2007). Neural
454 correlates of reexperiencing, avoidance, and dissociation in PTSD: Symptom
455 dimensions and emotion dysregulation in responses to script-driven trauma imagery.
456 *Journal of Traumatic Stress* 20, 713–725.
- 457 46. Krystal, H. (1971). Trauma: considerations of its intensity and chronicity.
458 *International Psychiatry Clinics* 8, 11–28.
- 459 47. Krystal, H. (1978). Trauma and affects. *Psychoanal Study Child* 33, 81–116.
- 460 48. Nestler, E.J. (2015). Δ FosB: A transcriptional regulator of stress and antidepressant
461 responses. *European Journal of Pharmacology* 753, 66–72.
- 462 49. Pearce, J.M., and Hall, G. (1980). A model for Pavlovian learning: Variations in the
463 effectiveness of conditioned but not of unconditioned stimuli. *Psychological Review* 87,
464 532–552.
- 465

466



467

468 Figure 1 – David Marr's Levels of Analysis for computational neuroscience as applied to

469 PTSD. (A) Definition of the three levels of analysis from ref. 7. (B) Application of those

470 levels to associative learning (left) and non-associative learning (right) in PTSD. (left)

471 Associative learning is a well-characterized system with a clear computational goal of

472 ethological relevance (Computational), a mathematically defined formal model

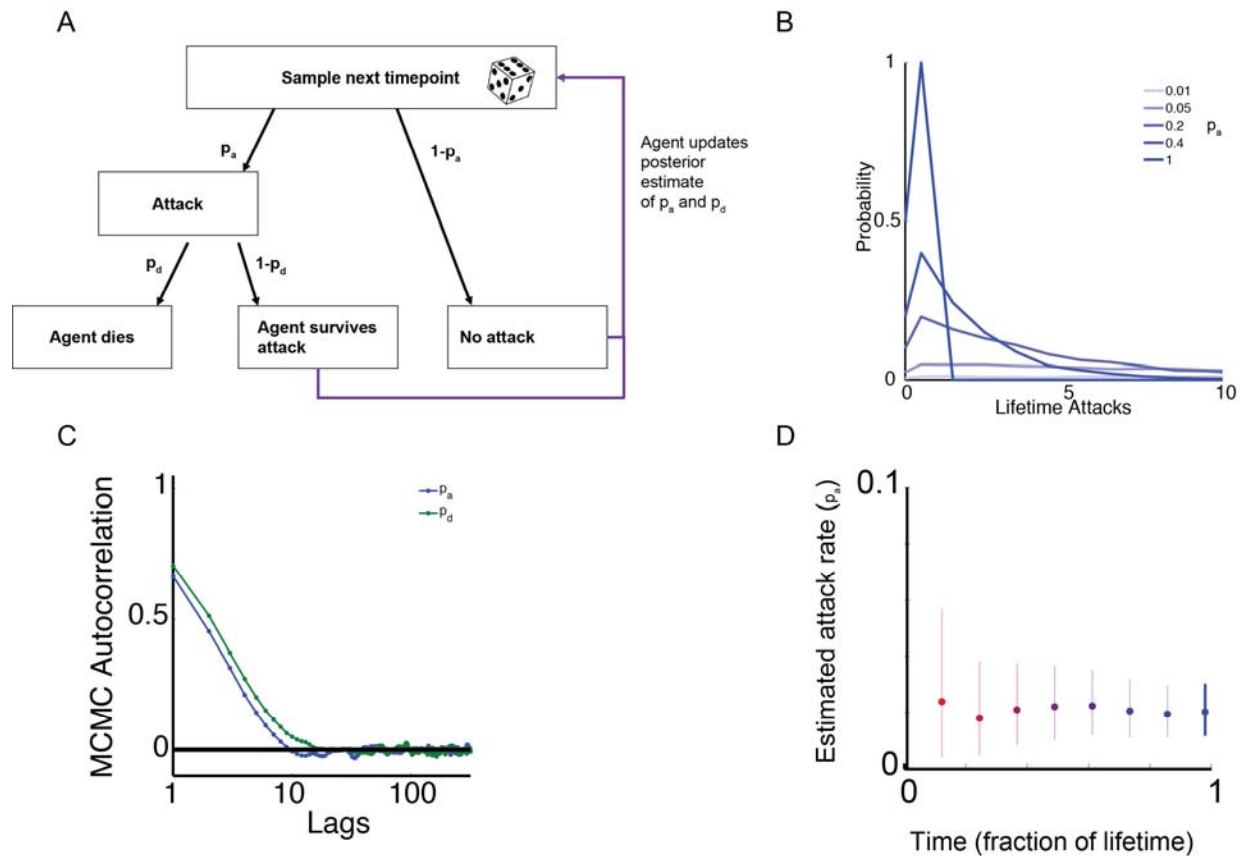
473 (Algorithm), and neural circuit mechanisms (Implementation). (right) Non-associative

474 learning is less well-understood. The goal posited here is that it's purpose is to predict

475 threats based on repetition of traumatic events (Computational). Schematized models

476 exist (Algorithmic) but lack a formal mathematical model, and the neurobiological

477 correlates of this are not fully understood (Implementation).



478

479 Figure 2 - A Bayesian observer can measure the rate of traumatic attacks. (A)

480 Schematic of a simplified doubly stochastic model of attacks (i.e., traumatic events).

481 Attacks occur randomly at each timepoint with a fixed probability p_a . Conditional on

482 attacks occurring, agents die with probability p_d . If agents survive, they estimate the

483 ongoing probability of attacks according to Bayes' rule. (B) Agents must estimate p_a and

484 p_d in an information-poor environment. The number of attacks experienced by the

485 typical agent is low, usually 3-5 over the course of a lifetime for $p_a=0.2$, a typical value

486 for the lethality of predator attacks (30). (C) The Bayesian estimator of the posterior

487 estimates of p_a and p_d for a typical example sequence of attacks ($p_a = 0.01, p_d = 0.2$)

488 shows convergence for p_a (blue) and for p_d (green). The autocorrelation of the MCMC

489 sampler goes to zero rapidly at long timelags for both parameters, demonstrating

490 convergence in the MCMC sampler. (D) As the agent continues over its lifetime (red to
491 blue map), the estimate of p_a slowly narrows (vertical lines, 95% intervals). Greater time
492 allows the agent to accumulate greater evidence about the true value of p_a .

493

494

495

496

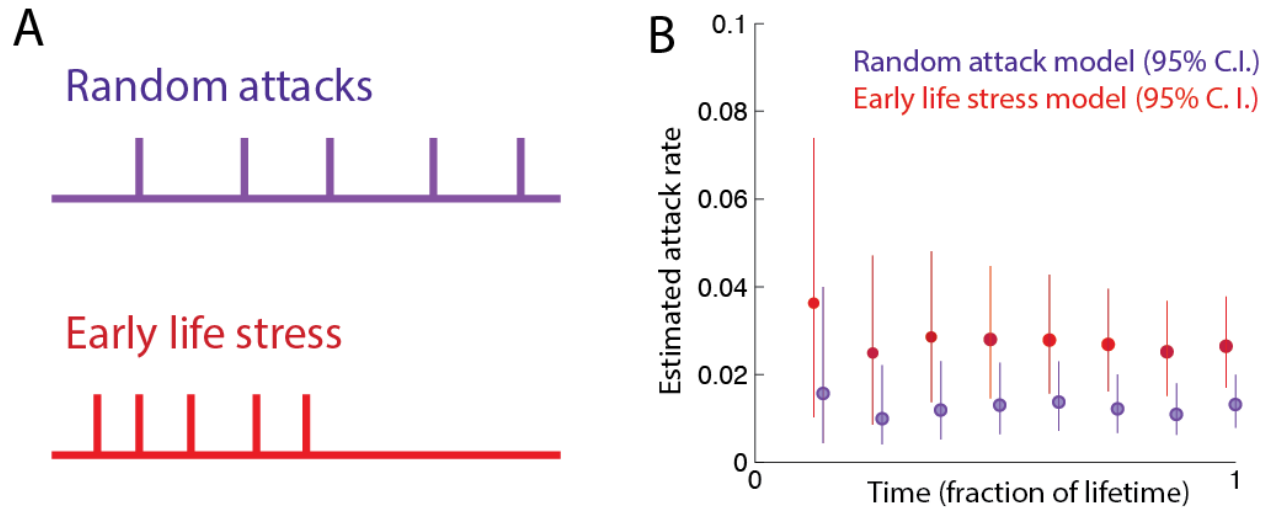
497

498

499

500

501



502

503 Figure 3 – Early life traumas have a disproportionate effect on the estimated attack rate.

504 (A) Characteristic examples of two distributions of attack frequencies. In the random

505 attack model, attacks are uniformly distributed across the lifespan. In the early life stress

506 (ELS) model, an identical number of attacks are uniformly distributed across the first

507 half of the lifespan. (B) Bayesian agents' posterior distributions for attack rate

508 sequentially measured across the lifespan, for the random and early attack models (p_a

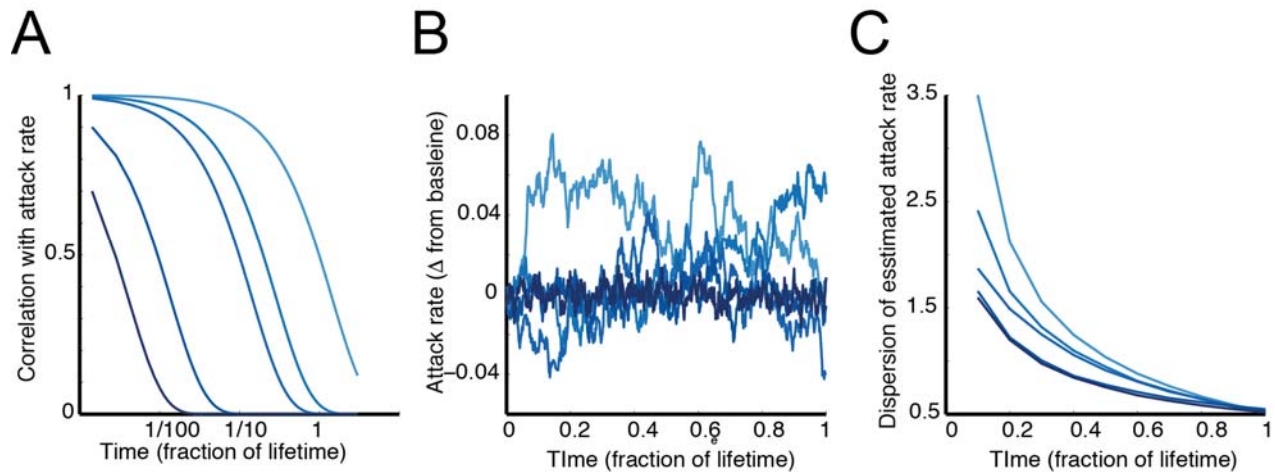
509 = 0.01 and $p_d = 0.2$). The discrepancy between estimated and true attack rate is

510 greatest at the start of life due to a higher density of attacks in the early life stress

511 model. Over the course of the lifespan, these two models arrive at similar estimates.

512

513



514

515

Figure 4 – Varying attack rates lead to misestimation of trauma rate. (A) Autoregressive

516

time series are random processes where adjacent timepoints are correlated according

517

to $x_t = cx_{t-1} + \mathcal{N}(0,0.1)$. The consequence of this is that the random attack rate x is

518

correlated across longer timescales, depending on the value of c . Timescales of

519

correlation are shown for five values of c , from lowest (dark blue) to highest (light blue).

520

(B) Example attack rates produced by such an autoregressive time series. (C) These

521

example attack rates can then be used to produce attack sequences for each c value,

522

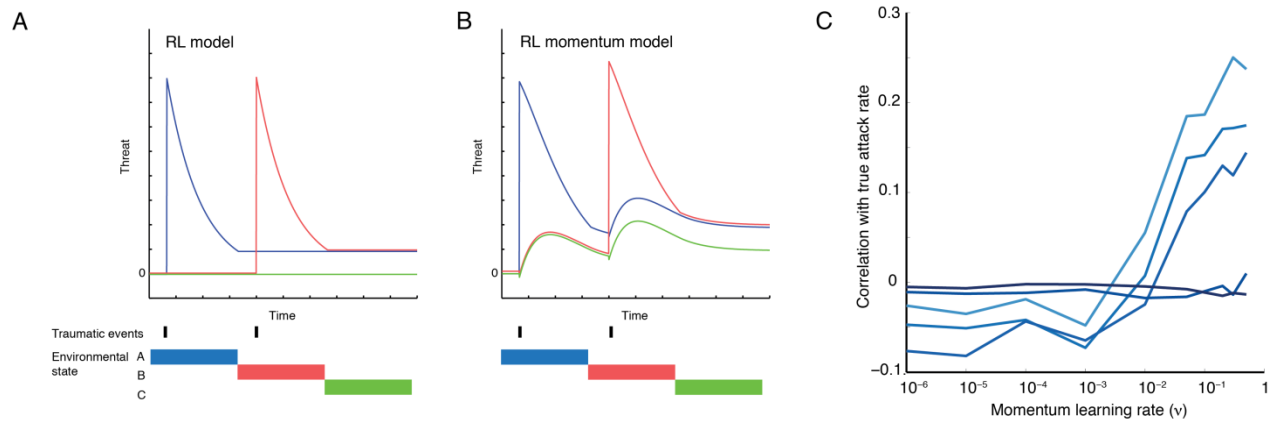
which can enable analysis of the performance of an optimal Bayesian agent. For

523

$n=10000$ simulations per autocorrelation (c) value, the error of estimated attack rates is

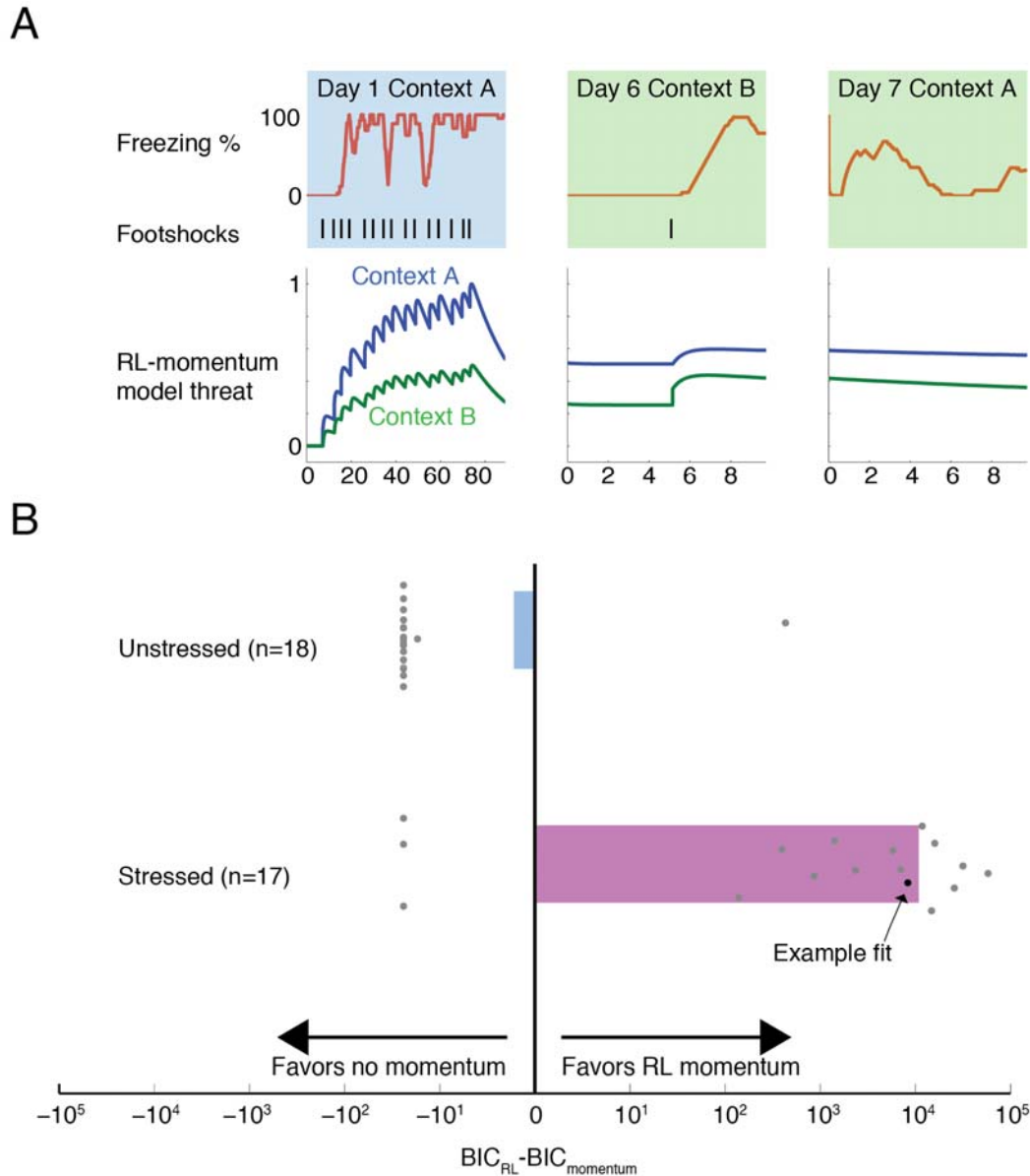
524

highest for long timescales of autocorrelation.



525
526 **Figure 5 – Reinforcement learning with momentum allows improved estimation of**
527 **autocorrelated attack rates. (A) Single traumatic events occur in different environmental**
528 **states (contexts), leading to increased associated threat according to the RL model. (B)**
529 **In the RL momentum model, the same series of attacks produces momentum which**
530 **ouples threat across contexts. Context C threat is due to momentum since the animal**
531 **receives no footshocks in that state. (C) The momentum learning rate term of the RL**
532 **momentum model enables extraction of information about fluctuating attack rates.**
533 **Autoregressive attack rates were produced as shown in figure 3 to produce n=10000**
534 **simulated attack sequences (light blue, highest autoregression to dark blue, lowest**
535 **autoregression). All attacks occur in a different context. In the absence of momentum,**
536 **the agent cannot extract information about fluctuations in underlying attack rate. With**
537 **higher momentum, the agent can extract information about the underlying attack rate**
538 **fluctuations.**

539
540
541
542



543

544 Figure 6 – RL momentum fits threat behavioral data in a mouse model of PTSD. (A)

545 Example mouse behavioral data across three days of in the stress-enhanced fear

546 learning model of PTSD (upper), along with RL momentum fit to behavioral data (lower).

547 (upper left) Freezing across 90 minutes (red) of exposure to 15 unpredictable

548 footshocks (black; 1mA, 1s). (upper center) Freezing across subsequent exposure to 1

549 uncued footshock in a new context. (upper right) Freezing during re-test in the new

550 context (lower left) Threat according to maximum likelihood model fit of the RL

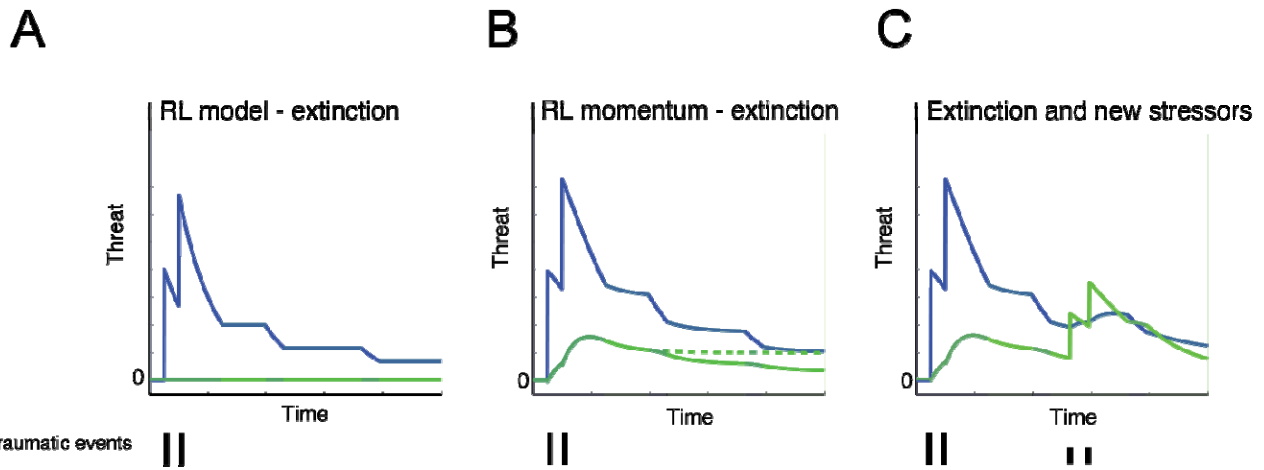
551 momentum model (threat associated with context A – blue, context B- green) on day 1,
552 (lower center) day 6, and (lower right) day7. (B) Model comparison between classic RL
553 model and RL momentum model for SEFL mice (n=17 stressed, n=18 controls). Bayes
554 information criterion (BIC) was calculated (see Methods) for maximum likelihood fits of
555 the RL model and RL momentum model for either unstressed animals (0 shocks on day
556 1) or stressed animals (15 shocks on day 1). Difference in BIC between the two models
557 is shown for individual animals (gray dots; black dot for example data from (A)), mean
558 BIC difference per condition as bars (blue – unstressed, pink – stressed).

559

560

561

562



563

564 Figure 7 – RL momentum model offers a new perspective on mechanisms of extinction

565 and symptom exacerbation in PTSD. (A) RL model: Two traumatic events in an initial

566 context (context A; blue highlight) produce threat learning associated with that context

567 (blue line) but no threat associated with a novel context (context B; green line) during

568 exposure to that context (green highlights). Extinction occurs when exposure to the

569 initial context A after the traumatic events causes threat prediction errors which

570 decrease threat associated with context A (blue highlights, second and third exposures).

571 (B) RL momentum model: Two traumatic events in initial context produce a momentum

572 which increases threat in a novel context (green line). Re-exposure to initial threat

573 context (context A; blue highlights) reduces threat associated with context A (blue line)

574 but also reduces threat momentum (green line). Green dotted line shows counterfactual

575 threat momentum if no re-exposure to context A had occurred). (C) RL momentum

576 model demonstrates a novel explanation for relapse during exposure therapy. Exposure

577 to smaller stressors (small lines) in a novel context increases threat associated with

578 context B (green line) but also, via the momentum term, increases threat associated

579 with the initial traumatic context A (blue line).